

Coulomb blockade of strongly coupled quantum dots studied via bosonization of a channel with a finite barrier

John M. Golden and Bertrand I. Halperin

Department of Physics, Harvard University, Cambridge, MA 02138

(22 August 2001)

A pair of quantum dots, coupled to each other through a point contact, can exhibit Coulomb blockade effects that reflect the presence of an oscillatory term in the dots' total energy whose value depends on whether the total number of electrons on the dots is even or odd. The effective energy associated with this even-odd alternation is reduced, relative to the bare Coulomb blockade energy U_ρ for uncoupled dots, by a factor $(1 - f)$ that decreases as the interdot coupling is increased. When the transmission coefficient for interdot electronic motion is independent of energy and is the same for all channels within the point contact (which are assumed uncoupled), the factor $(1 - f)$ takes on a universal value determined solely by the number of channels N_{ch} and the dimensionless conductance g of each individual channel. When an individual channel is fully opened (the limit $g \rightarrow 1$), the factor $(1 - f)$ goes to zero.

When the interdot transmission coefficient varies over energy scales of the size of the bare Coulomb blockade energy U_ρ , there are corrections to this universal behavior. Here we consider a model in which the point contact is described by a single orbital channel containing a parabolic barrier potential, with ω_P being the harmonic oscillator frequency associated with the inverted parabolic well. We calculate the leading correction to the factor $(1 - f)$ for $N_{\text{ch}} = 1$ (spin-split) and $N_{\text{ch}} = 2$ (spin-degenerate) point contacts, in the limit where g is very close to 1 and the ratio $2\pi U_\rho / \hbar \omega_P$ is not much greater than 1. Calculating via a generalization of the bosonization technique previously applied in the case of a zero-thickness barrier, we find that for a given value of g , the value of $(1 - f)$ is increased relative to its value for a zero-thickness barrier, but the absolute value of the increase is small in the region where our calculations apply.

PACS: 73.23.Hk, 73.63.Kv, 71.10.Pm, 72.10.-d

I. INTRODUCTION

In recent years, there have been a number of theoretical and experimental studies of the manner in which Coulomb blockade effects in a metallic particle or semiconductor quantum dot disappear when the conducting island becomes more electrically connected to its environment.¹⁻¹¹ Here we focus on a system in which two symmetric quantum dots are defined by applying negative voltages to gate electrodes that lie on the surface of a semiconductor heterostructure above a two-dimensional electron gas (2DEG). We assume that the dots are joined by a quantum point contact containing a single orbital channel that is almost perfectly transmitting at the Fermi energy, but that the dots are isolated from their respective leads by comparatively large tunnel barriers. In this geometry, information about the Coulomb blockade energy U_ρ involved in the transfer of electrons from one dot to the other can be obtained by observing the positions of Coulomb blockade peaks in the conductance across the entire system (from one lead to another) when that conductance is plotted as a function of voltages on gates coupled to each of the dots.¹⁻³

Previous analyses of the disappearance of the Coulomb blockade for two-dot systems¹² containing such a partially open point contact have characterized the contact by a number N_{ch} of degenerate one-dimensional (1D) channels and by the dimensionless conductance g of each

channel (where $0 \leq g \leq 1$).⁶⁻⁹ This characterization is complete in the limit where the electronic transmission amplitude through the contact is independent of energy for electron energies that differ from the Fermi energy by no more than an amount comparable to U_ρ . The energy independence of the transmission amplitude means that this characterization corresponds to a potential barrier which is sufficiently thin that it can be modeled as a delta function. Because the Coulomb blockade energy U_ρ is much smaller than the Fermi energy E_F , working in this "delta-function barrier limit" can yield good results even though the product of the barrier width and the Fermi wave vector k_F is generally much greater than 1 (with k_F being the value of the Fermi wave vector in the 2DEG far from the barrier).

Nevertheless, it seems important to investigate further the consequences of relaxing the assumption of a delta-function barrier limit. For one thing, it is possible to generate wider barriers using an appropriate gate geometry, and one would like to understand at what point the delta-function-limit calculations break down. Secondly, estimating the corrections due to a barrier's finite thickness provides a valuable check on the delta-function-limit results.

Another reason for interest is that recent experiments on transmission through quantum point contacts have shown unexpected structure (e.g., an apparent conductance plateau near $0.7(2e^2/h)$ at intermediate tempera-

tures¹³) whose origin is only poorly understood. Such results suggest that transmission through a point contact may have a nontrivial energy dependence, and such a dependence could well have an effect on the breakdown of the Coulomb blockade in the coupled-dot geometry. With the aim of explaining such effects in mind, it is a helpful first step to study theoretically the effects of energy dependences in a simpler situation where the barrier potential is known and many-body effects are reduced to a bare minimum. In this vein we consider here a model in which the two dots are separated by a parabolic barrier of nonzero width and the electron-electron interaction is taken to be constant for any two electrons located anywhere on the same quantum dot.

This model presents challenges for “bosonization techniques” that characterize point-contact constrictions as one-dimensional fermionic seas whose low-energy degrees of freedom can be expressed in terms of bosonic density and phase variables.^{14–18} In such “bosonized” models, the behavior of incompletely opened channels is commonly studied by introducing a zero-width delta-function barrier at a specific point in the one-dimensional sea.^{4,5,20,21} By way of contrast, this paper seeks to show how a bosonized model of a one-dimensional system can describe the single-particle effects of replacing a delta-function barrier with a barrier that more realistically corresponds to a finite-length constriction—i.e., a barrier of nonzero width and therefore nontrivial single-particle transmission properties.

Before proceeding, we should describe more fully what is already understood about systems of two symmetric quantum dots connected by a single orbital channel containing degenerate spin modes. In such systems, an energy scale U_ρ characterizes the energy cost of moving electronic charges between different segments of the system. Moreover, the system’s Coulomb blockade behavior reflects the presence of an energy term proportional to U_ρ that oscillates between one value held when the total number of electrons on the dots is even and another value held when the total electron number is odd.^{1,8}

Previous work, both experimental and theoretical, has shown that as the conductance of the interdot point contact is increased, the energy scale associated with this even-odd alternation is reduced by a factor of $(1 - f)$, where f goes to 1 when the channel is fully open. When the transmission coefficient for electronic motion within this channel is independent of energy (i.e., the delta-function barrier limit), the factor $(1 - f)$ takes on a universal value determined solely by the number of point contact channels N_{ch} (the channels being assumed degenerate and uncoupled) and the dimensionless conductance g of each individual channel (If G is the total conductance of the point contact, $g = G/N_{\text{ch}}(e^2/h)$). We refer to the value f in the factor $(1 - f)$ as the *fractional peak splitting* because it has been measured by observing the relative separation of conductance peaks in a series of Coulomb blockade experiments.^{1–3,8}

This paper studies the corrections to f , and therefore

to $(1 - f)$, that result when the assumption of a delta-function barrier limit is relaxed—in other words, when the interdot barrier is more realistically treated as having a finite height and nonzero width. A prior study of the effects of a nonzero-width barrier concentrated on the limit of weakly coupled dots (the limit $g \rightarrow 0$).¹⁰ This study revealed that, if the one-dimensional channels between two dots, or between a dot and a lead, contain a tunneling barrier of finite height V_0 (in energy units) and of nonzero width ξ , the behavior of such systems is responsive to another energy scale, W , that characterizes the energy range (for electrons incident on the barrier) over which the probability of transmission through the barrier varies substantially.¹⁰ For relatively large and shallow dots, such as those that have been constructed in GaAs/AlGaAs heterostructures at low temperatures,^{1–3} the energies U_ρ and W tend to be much smaller than the Fermi energy E_F but much larger than both the single-particle level spacing δ and the thermal energy $k_B T$. As a result, such systems are characterized by the following hierarchy of energy scales:¹⁰

$$k_B T, \delta \ll U_\rho \lesssim W \ll E_F. \quad (1)$$

Because W is comparable in size to the intermediate energy scale U_ρ (which acts as a kind of “excitation energy scale” with respect to independent-particle energies), effects from the barrier’s finite size can be significant and deserve investigation before they are confidently discarded.

Our prior study of the weak-coupling limit where $g \ll 1$ found that the finiteness of the barrier leads to an upward correction to the universal f -versus- g curve for a delta-function barrier. In other words, for a given *small* value of g , the fractional peak splitting f is enhanced relative to its value for a delta-function barrier.¹⁰ This enhancement occurs because, in a channel containing a barrier with a finite energy height (as opposed to a delta-function barrier), electrons can tunnel from one dot to another through largely unreflected states that have single-particle energies greater than the energy that corresponds to the finite barrier’s peak.¹⁰

In order to study the correction to the universal f -versus- g curve, in our prior work we made several basic assumptions about the system of two symmetric dots connected by a single orbital channel. First, we assumed that the electrons that enter the point contact between the dots are in the lowest energy eigenstate for motion perpendicular to the channel and can therefore be described by a one-dimensional (1D) Schrödinger equation with an effective barrier potential $V(x)$. We assumed that $V(x)$ could be treated as parabolic, with a harmonic oscillator frequency ω_P associated with the inverted parabolic well. (In this case, the transmission energy scale W is given by $\hbar\omega_P/2\pi$.) In addition, we assumed that, despite the nonzero width of the barrier, the essential nature of electron-electron interactions was still accurately represented by the standard Coulomb blockade model, in

which the interaction energy of a quantum dot is analogous to that of a classical capacitor—i.e., proportional to the charge on the dot squared. Having made these assumptions, we found that, in the limit $g \rightarrow 0$, the leading behavior of the enhancement to f is roughly proportional to $N_{\text{ch}}(2\pi U_\rho/\hbar\omega_P)/|\ln g|$. For the experimental systems with which we are concerned, where N_{ch} is 1 or 2 and where $2\pi U_\rho/\hbar\omega_P \simeq 1$, the size of the enhancement is relatively small.¹⁰

This paper extends study of such finite-barrier corrections to the strong-coupling limit where $(1-g) \ll 1$. In doing so, we repeat the two assumptions described above. The assumption of a parabolic form for the imposed barrier potential is likely as good as before.^{21,22} However, our simplistic treatment of the electron-electron interactions is likely less firm, given that the point contact is now largely open and therefore much more likely to be occupied by electrons interacting in a way not reflected by the standard capacitive Coulomb blockade model. Nonetheless, because the barrier region is still small in relation to the larger conducting basins of the two dots, and because the effects from a combination of the Coulomb blockade model and the interdot barrier's finite size are themselves sufficiently interesting and complex, in this initial stab at the problem of finite barriers we ignore the effects of interactions specific to the point contact, with the understanding that separate efforts to understand those effects should follow.

Thus, the basic parameters for our strong-coupling study are the same as those for the weak-coupling limit. The N_{ch} degenerate spin channels are assumed to contain effectively identical barriers, and the interdot barrier can be modeled as fully parabolic so long as we are concerned only with energies within a restricted range about the barrier peak. We therefore describe the single interdot orbital channel as containing the potential:

$$\begin{aligned} V(x) &= V_0(1 - x^2/2\xi^2) & \text{for } |x| < \sqrt{2}\xi \\ V(x) &= 0 & \text{for } |x| \geq \sqrt{2}\xi. \end{aligned} \quad (2)$$

See Figure 1. As we will later see, our ultimate results are independent of the potential's details away from the barrier peak. Key aspects of the barrier potential are the “depth” ($E_F - V_0$) of its peak relative to the Fermi surface and the harmonic oscillator frequency $\omega_P = \sqrt{V_0/m\xi^2}$ associated with the inverted parabolic well.¹⁰ (Note that $\hbar\omega_P/E_F \approx \sqrt{2}(k_F\xi)^{-1}$, which is assumed to be much less than 1.)

We use the single-particle eigenfunctions that correspond to the above potential to calculate corrections to f . To do so, we incorporate these eigenfunctions in a generalization of a bosonization approach^{14–19} that was used earlier in the delta-function barrier limit.^{4–9} We first find the change in the two-dot system's ground state energy as the value of $(1-g)$ is increased from zero. This energy shift $\Delta(\rho)$ is a function of $(1-g)$ and another dimensionless quantity ρ , which represents a linear combination of the gate voltages applied to the two dots.^{8,9} When the

total number of electrons on the two dots is even, the fractional peak splitting f is given by the following formula:

$$f = 1 - \frac{\Delta(1) - \Delta(0)}{U_\rho/4}. \quad (3)$$

By applying this formula, we find that, consistent with our earlier conjecture,¹⁰ for both $N_{\text{ch}} = 1$ and $N_{\text{ch}} = 2$ the leading finite-barrier corrections *decrease* the value of f observed for a given value of g when g is close to 1. For $2\pi U_\rho/\hbar\omega_P \lesssim 2$ and $(1-g) \ll 1$, the magnitude of the decrease is proportional to $(2\pi U_\rho/\hbar\omega_P)/|\ln(1-g)|$ for $N_{\text{ch}} = 1$ and to $(2\pi U_\rho/\hbar\omega_P)\sqrt{1-g}\{1 - |\ln(1-g)|^{-1}\}$ for $N_{\text{ch}} = 2$.

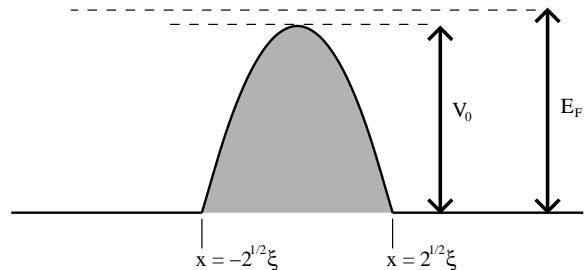


FIG. 1. A schematic representation of the 1D model for a parabolic barrier between two quantum dots. The half width of the barrier at half maximum is ξ , and the potential energy at the barrier's peak is V_0 , which is less than, but comparable in size to, the Fermi energy E_F .

In Sec. II, we show how to use the bosonization approach to derive an effective action that captures the Coulomb blockade behavior of such a system for an arbitrary number N_{ch} of interdot tunneling channels. In Sec. III, we use the effective action of Sec. II to solve for the leading f -versus- g behavior for $N_{\text{ch}} = 1$ and $g \simeq 1$. In Sec. IV, we do the same for $N_{\text{ch}} = 2$. In Sec. V, we remark on the significance and limitations of our results.

II. BOSONIZATION WITH A BARRIER OF FINITE WIDTH

To calculate the corrections due to the interdot barrier's nonzero width, we start with a fermionic formulation of our system of two symmetric quantum dots connected by a single orbital channel containing an arbitrary number N_{ch} of degenerate spin modes. Since this fermionic problem is effectively one-dimensional,¹⁰ we can apply to it a variation of the standard technique of bosonization.^{4,5} Having “bosonized” the problem, we integrate out various bosonic degrees of freedom to obtain a low-energy effective action involving only a single set of scalar fields.

The fermionic formulation of the problem of coupled quantum dots is quite straightforward.^{4,5,7–9} In a basis of

non-interacting single-particle eigenstates, the fermionic Hamiltonian consists of a kinetic-energy part H_K and a charging-energy part H_C :

$$\begin{aligned} H_K &= \sum_{\sigma} \sum_{\zeta} \int dk \xi_k a_{k\sigma\zeta}^{\dagger} a_{k\sigma\zeta} \\ H_C &= U_{\rho}(\hat{n} - \rho/2)^2, \end{aligned} \quad (4)$$

where ξ_k is the energy of the single-particle eigenstate; σ is the channel index; ζ is the index for states incident on the barrier from the left ($\zeta = 1$) and the right ($\zeta = -1$), respectively; and $k_F + k$ is the magnitude of the wave vector associated with motion along the one-dimensional channel (k_F is the Fermi wave vector and $|k|$ is assumed to be smaller than k_F). The operator \hat{n} measures the difference between the number of electrons to the right of the barrier and the number of electrons to the left of the barrier. If one lets \hat{n}_1 be the occupation number for the left dot and \hat{n}_2 be the occupation number for the right dot, $\hat{n} = (\hat{n}_2 - \hat{n}_1)/2$. In order to determine the value of f via Eq. 3, we consider the case where the total number of electrons on the two dots is even, so that \hat{n} is an operator with integer eigenvalues. (When the total number of electrons is odd, \hat{n} has half-integer eigenvalues.)

The operator \hat{n} can be written in terms of fermionic position operators $\psi_{\sigma}^{\dagger}(x)$ and $\psi_{\sigma}(x)$ as follows:

$$\hat{n} = \frac{1}{2} \sum_{\sigma} \int dx [\Theta(x) - \Theta(-x)] \psi_{\sigma}^{\dagger}(x) \psi_{\sigma}(x), \quad (5)$$

where $\psi_{\sigma}(x)$ consists of left-incident and right-incident parts,

$$\psi_{\sigma}(x) = \psi_{\sigma 1}(x) + \psi_{\sigma, -1}(x), \quad (6)$$

and where $\Theta(x)$ is a Heaviside step function centered on the dividing line between the “right” and “left” sides of the barrier at $x = 0$.

If one were bosonizing fermionic operators associated with a basis of plane-wave states, one could bosonize the above Hamiltonian by using the standard formula:

$$\psi_{\sigma\zeta}(x) = \frac{1}{\sqrt{2\pi\alpha}} e^{i\zeta k_F x} e^{i\sqrt{\pi}[\zeta\theta_{\sigma}(x) + \phi_{\sigma}(x)]}, \quad (7)$$

where $\theta_{\sigma}(x)$ and $\phi_{\sigma}(x)$ are scalar boson fields and α is a quantity analogous to a lattice spacing that is used to impose an ultraviolet cutoff at energies approximating $\hbar v_F/\alpha$ on the bosonic degrees of freedom^{14–19} (α is ultimately meant to be taken to zero—a limit that can be reasonably taken when $E_F \gg U_{\rho}$ and the approach to modeling the double-dot system can be supposed to work down to length scales a , where $\hbar v_F/a$ is much greater than the relevant excitation scale U_{ρ}). The annihilation operators associated with the plane-wave states would then be given by the equation:

$$a_{k\sigma\zeta} = \frac{1}{2\pi\sqrt{\alpha}} \int dx e^{-i\zeta kx} e^{i\sqrt{\pi}[\zeta\theta_{\sigma}(x) + \phi_{\sigma}(x)]}. \quad (8)$$

In terms of this plane-wave bosonization scheme, the operator \hat{n} could be simply expressed in terms of the boson fields⁴:

$$\hat{n} = \frac{1}{\sqrt{\pi}} \sum_{\sigma} \theta_{\sigma}(0). \quad (9)$$

Unfortunately, our problem is not so simple. The basis of single-particle states that appears in Eq. 4 is not a plane-wave basis. The eigenstates are those of a one-dimensional system containing a barrier of finite height and nonzero width, and they therefore include incident, reflected, and transmitted parts.

Happily, the kinetic-energy part of the Hamiltonian H_K does not concern itself with such complications. So long as the single-particle level spacing can be treated as effectively zero, we can proceed with regard to H_K just as if the single-particle states were plane waves. Accordingly, if we focus on bosonizing H_K , we can bosonize the annihilation operators in Eq. 4 in the same way as in Eq. 8. Under this bosonization scheme, the kinetic energy H_K has the following standard form:

$$H_K = \frac{v_F}{2} \sum_{\sigma} \int dx \left\{ [\partial_x \phi_{\sigma}(x)]^2 + [\partial_x \theta_{\sigma}(x)]^2 \right\}. \quad (10)$$

Our next task is to find a proper bosonized form for the position operators $\psi_{\sigma\zeta}(x)$ that appear in Eq. 5. Recalling that we already have bosonized forms for the operators $a_{k\sigma\zeta}$, we express the $\psi_{\sigma\zeta}(x)$ in bosonized form by using the fact that the position operators consist of linear combinations of the operators $a_{k\sigma\zeta}$. In particular, in the continuum limit,

$$\psi_{\sigma\zeta}(x) = \int dk Y_{k\zeta}(x) a_{k\sigma\zeta}, \quad (11)$$

where the functions $Y_{k\zeta}(x)$ are the single-particle eigenfunctions of the non-interacting one-dimensional system.²³ For the potential described by Eq. 2, we have derived these $Y_{k\zeta}(x)$ in prior work, using the fact that there are exact solutions (parabolic cylinder functions) to the Schrödinger equation for a single particle in a parabolic potential.¹⁰ Using the $Y_{k\zeta}(x)$, we find that, to leading order in the perturbation due to the barrier, \hat{n} equals $\hat{n}_0 + \delta\hat{n}$, where

$$\begin{aligned} \hat{n}_0 &= \frac{-1}{4\pi i} \sum_{\sigma} \sum_{\zeta} \zeta \int dk_1 \int dk_2 \\ &\quad \times \left(\frac{1}{k_2 - k_1 + i\eta} + \text{c.c.} \right) a_{k_2\sigma\zeta}^{\dagger} a_{k_1\sigma\zeta} \\ \delta\hat{n} &= \frac{1}{2\pi} \sum_{\sigma} \int dk_1 \int dk_2 R(\epsilon_1, \epsilon_2) \\ &\quad \times \left\{ \frac{e^{i[D(\epsilon_2) - D(\epsilon_1)]}}{k_2 - k_1 + i\eta} a_{k_1\sigma 1}^{\dagger} a_{k_2\sigma, -1} + \text{h.c.} \right\}, \end{aligned} \quad (12)$$

where “c.c.” and “h.c.” stand, respectively, for the complex conjugate and hermitian conjugate of the preceding term, and the following identities hold:

$$\begin{aligned}\epsilon_i &= \epsilon_F + v_F k_i / \omega_P \\ R(\epsilon_1, \epsilon_2) &= \frac{e^{-\pi\epsilon_1} + e^{-\pi\epsilon_2}}{2\sqrt{1 + e^{-2\pi\epsilon_1}} \sqrt{1 + e^{-2\pi\epsilon_2}}} \\ D(\epsilon) &= \frac{\arg \Gamma(1/2 - i\epsilon) - \epsilon + \epsilon \ln |\epsilon|}{2} + C, \quad (13)\end{aligned}$$

with C being a constant independent of ϵ and $\epsilon_F = \frac{E_F - V(0)}{\hbar\omega_P}$ being the value of ϵ at the Fermi energy.²⁴

In the above equations, the dimensionless variables $\epsilon_i = \frac{E_i - V(0)}{\hbar\omega_P}$ measure the energy distance from the finite barrier’s peak.¹⁰ The scale for these dimensionless energy measures is the harmonic oscillator energy $\hbar\omega_P$, and in terms of these dimensionless measures

$$1 - g = \frac{1}{1 + e^{2\pi\epsilon_F}}. \quad (14)$$

The functions $R(\epsilon_1, \epsilon_2)$ and $D(\epsilon_i)$ are associated with the single-particle transmission properties of the barrier. Each additive term in $R(\epsilon_1, \epsilon_2)$ is a product of transmission and reflection amplitudes, reflecting the fact that the leading contributions to $\delta\hat{n}$ come from “overlaps” between the transmitted part of an original right-mover and the reflected part of an original left-mover and vice versa). Meanwhile, $D(\epsilon_i)$ represents a phase associated with the scattering of a single-particle wavefunction. Because of the exponential growth (or damping) of $R(\epsilon_1, \epsilon_2)$, we should not be surprised to find that $R(\epsilon_1, \epsilon_2)$ plays a starring role in the nature of our leading-order result—whereas, to first approximation, contributions from $D(\epsilon_i)$ will prove to be negligible.

Before we proceed further, we should make three remarks about Eq. 12. First, we should note that derivation of the above equation for $\delta\hat{n}$ ignores contributions to \hat{n}_0 from integrating over some interior portion of the barrier region in which approximating the single-particle wavefunctions by plane waves, or at least by WKB approximations to plane waves, is no longer valid. Hence—because the exact eigenfunctions in the barrier region (parabolic cylinder functions) do not “explode” in amplitude as one goes further toward the center of the barrier²⁵—as in our derivation of analogous identities in the limit of weakly coupled dots,¹⁰ we expect additive corrections of rough order ξ to the Eq. 12 cofactors $\frac{1}{k_2 - k_1 \pm i\eta}$. Consequently, to avoid substantial corrections to Eq. 12, we must be able to restrict our attention to wave-vectors k_i (measured from the appropriate Fermi wave vector in one dimension) such that

$$|k_i| \xi \lesssim 1. \quad (15)$$

Because the exponentially variant function $R(\epsilon_1, \epsilon_2)$ strongly favors values of k_i that correspond to ϵ_i near 0, the k_i of most interest for calculating corrections to the

universal behavior are those for which $k_i \simeq -\omega_P \epsilon_F / v_F$. The above restriction on k_i can thus be seen to mean that we need $\epsilon_F \lesssim \sqrt{2E_F/V_0}$. For systems (such as those this paper seeks to model) in which $E_F/V_0 \simeq 1$, the restriction then reduces (conservatively speaking) to $\epsilon_F \lesssim 1$ or, equivalently, $(1 - g) \gtrsim 10^{-3}$. Given that the relevant experiments with quantum dot systems¹⁻³ have generally not resolved g to increments of 10^{-3} , this constraint is not a serious one.

As a second point regarding Eq. 12, it should be noted that, for $\epsilon_F \lesssim 1$, this intermediate result (and therefore those that follow from it) is insensitive to details of the barrier away from the barrier peak (e.g., the slope discontinuities that occur in our barrier potential at $x = \pm\sqrt{2}\xi$) so long as ξ is large compared to the inverse Fermi wave vector k_F^{-1} (with the Fermi wavelength itself being of the order of $2\pi\hbar/\sqrt{2mV_0}$, the wavelength associated with the peak barrier energy, V_0). The condition $\xi \gg k_F^{-1}$ is typically true of the kinds of quantum dots that have motivated these investigations.^{1-3,10}

A third remark about Eq. 12 is that in deriving $\delta\hat{n}$, we have ignored a correction involving terms of the form $(\cos[D(\epsilon_2) - D(\epsilon_1)] - 1)/(k_2 - k_1 \pm i\eta)$. We ignored similar “phase-based” terms in Ref. 10. The basic reason that we ignore these terms here derives from the fact that, because the characteristic excitation energy U_ρ is less than $\hbar\omega_P$, the variation of the numerator of these terms over any region of particular interest should be very small. As a result, in the regions that we generally find to be most important (those regions near the simple poles where $k_2 = k_1 \pm i\eta$ and the magnitudes of other contributing terms tend toward infinity), these phase-based terms go to zero. Thus, we have good reason to expect that the contribution from these phase-based terms is small compared to the contribution from the terms we keep. Indeed, if we follow the calculation of the lowest-order contribution from these terms further, we would find that, by reasoning parallel to that used in Sec. III to perform various wave vector integrals, these terms produce a contour integral with no contribution from residues of the simple poles at $k_2 = k_1 \pm i\eta$ and only negligible, higher-order contributions from integration around other singularities and branch cuts.

Returning to Eq. 12 and the process of determining the fractional peak splitting, we observe that if the operators $a_{k\sigma\zeta}$ were annihilation operators for particles in plane-wave states (e.g., if there were no interdot barrier), \hat{n} would simply equal \hat{n}_0 . In other words, \hat{n}_0 bears the same relation to the bosonic fields associated with the barrier-state operators $a_{k\sigma\zeta}$ that \hat{n} bears to the bosonic fields associated with the similarly indexed plane-wave operators of Eq. 8. From Eq. 9, it therefore follows that

$$\hat{n}_0 = \frac{1}{\sqrt{\pi}} \sum_{\sigma} \theta_{\sigma}(0). \quad (16)$$

We do not have a similarly simple formula for $\delta\hat{n}$. Substituting for the operators $a_{k\sigma\zeta}$, we find that

$$\begin{aligned} \delta\hat{n} = & \frac{1}{(2\pi)^3\alpha} \sum_{\sigma} \int dx_1 \int dx_2 \int dk_1 \int dk_2 R(\epsilon_1, \epsilon_2) \\ & \times \left\{ \frac{e^{i[D(\epsilon_2)-D(\epsilon_1)]} e^{i(k_1x_1+k_2x_2)}}{k_2 - k_1 + i\eta} e^{-i\sqrt{\pi}[\theta_{\sigma}(x_1)+\phi_{\sigma}(x_1)]} \right. \\ & \left. \times e^{-i\sqrt{\pi}[\theta_{\sigma}(x_2)-\phi_{\sigma}(x_2)]} + \text{h.c.} \right\} \end{aligned} \quad (17)$$

Having now obtained bosonized expressions for the separate terms \hat{n}_0 and $\delta\hat{n}$, we express the Hamiltonian as a whole in bosonized form:

$$H = H_K + H_C^{(0)} + H_C^{(1)} + H_C^{(2)}. \quad (18)$$

H_K is given by Eq. 10, and the remaining terms are as follows:

$$\begin{aligned} H_C^{(0)} &= U_{\rho} \left[\frac{1}{\sqrt{\pi}} \sum_{\sigma} \theta_{\sigma}(0) - \rho/2 \right]^2 \\ H_C^{(1)} &= U_{\rho} \delta\hat{n} \left[\frac{1}{\sqrt{\pi}} \sum_{\sigma} \theta_{\sigma}(0) - \rho/2 \right] + \text{h.c.} \\ H_C^{(2)} &= U_{\rho} (\delta\hat{n})^2. \end{aligned} \quad (19)$$

The $H_C^{(2)}$ term can be dropped from the leading-order calculation because, to second-order in $\delta\hat{n}$ (which due to $R(\epsilon_1, \epsilon_2)$ is itself roughly proportional to $\sqrt{1-g}$ at the Fermi surface), $H_C^{(2)}$ contributes nothing to the ρ -dependence of the ground-state energy. Recall from Eq. 3 that it is the ρ -dependence of the ground-state energy that provides the basis for calculation of the fractional peak-splitting f .^{8,9}

To simplify calculation of this ρ -dependence, we shift the θ_{σ} -fields by a term linear in ρ : $\theta_{\sigma}(x) \rightarrow \theta_{\sigma}(x) + \sqrt{\pi}\rho/2N_{\text{ch}}$. This transformation leaves us with a Hamiltonian in which the ρ -dependence appears only in the perturbative factors of $\delta\hat{n}$. The transformed (and truncated) Hamiltonian has the following form:

$$\begin{aligned} H_K &= \frac{v_F}{2} \sum_{\sigma} \int dx \left\{ [\partial_x \phi_{\sigma}(x)]^2 + [\partial_x \theta_{\sigma}(x)]^2 \right\} \\ H_C^{(0)} &= \frac{U_{\rho}}{\pi} \left[\sum_{\sigma} \theta_{\sigma}(0) \right]^2 \\ H_C^{(1)} &= \frac{U_{\rho}}{\sqrt{\pi}} \sum_{\sigma} [\delta\hat{n} \theta_{\sigma}(0) + \theta_{\sigma}(0) \delta\hat{n}], \end{aligned} \quad (20)$$

where $\delta\hat{n}$ is now given by the identity:

$$\begin{aligned} \delta\hat{n} = & \frac{1}{(2\pi)^3\alpha} \sum_{\sigma} \int dx_1 \int dx_2 \int dk_1 \int dk_2 R(\epsilon_1, \epsilon_2) \\ & \times \left\{ \frac{e^{i[D(\epsilon_2)-D(\epsilon_1)]} e^{i(k_1x_1+k_2x_2)}}{k_2 - k_1 + i\eta} e^{-i\pi\rho/N_{\text{ch}}} \right. \\ & \times e^{-i\sqrt{\pi}[\theta_{\sigma}(x_1)+\phi_{\sigma}(x_1)]} \\ & \left. \times e^{-i\sqrt{\pi}[\theta_{\sigma}(x_2)-\phi_{\sigma}(x_2)]} + \text{h.c.} \right\} \end{aligned} \quad (21)$$

With Eq. 21, we have reached the end of the road with regard to the Hamiltonian approach. To progress further, we shift to an action-based, path-integral formulation. For ease of notation, we will henceforth assume that we have chosen units in which

$$\hbar = 1 \quad (22)$$

and drop \hbar from subsequent intermediate calculations (although we resuscitate it in stating our final results). Having made this choice of units, we proceed by integrating out various degrees of freedom: first, the ϕ -field degrees of freedom, and second, the θ -field degrees of freedom away from $x = 0$. The result is an effective action in terms of fields $\theta_{\sigma}^{(0)}(\tau)$ that are equivalent to the θ -field degrees of freedom at $x = 0$. This effective action, dependent only on the $x = 0$ degrees of freedom for the original θ -fields, is analogous, though—significantly—not equivalent, to that previously obtained for a system containing a delta-function barrier (see Refs. 1 and 2).

We do no more than outline the process of integrating out the ϕ -fields and θ -fields because the methodology for doing so is fairly straightforward. With regard to integrating out the ϕ -fields, a key point is that, in the path-integral approach, a Lagrangian term linear in $\partial_x \phi(x, \tau) \partial_{\tau} \theta(x, \tau)$ appears in the action (just as a $p\dot{x}$ -term appears in going from the Hamiltonian for a single particle to the corresponding Lagrangian). Having accounted for this term, we eliminate the ϕ -fields by performing a standard Gaussian integration. The result is an effective action entirely in terms of θ -fields.

Having obtained this effective action, we introduce the field $\theta_{\sigma}^{(0)}(\tau)$ and the auxiliary fields $\lambda_{\sigma}(\tau)$. We use the λ -fields to enforce the identity $\theta_{\sigma}(0, \tau) = \theta_{\sigma}^{(0)}(\tau)$ by adding to the action the following term:

$$S_{\lambda} = \sum_{\sigma} \int d\tau i\lambda_{\sigma}(\tau) \left[\theta_{\sigma}^{(0)}(\tau) - \theta_{\sigma}(0, \tau) \right]. \quad (23)$$

Having added S_{λ} to the action, we can substitute $\theta_{\sigma}^{(0)}(\tau)$ for $\theta_{\sigma}(0, \tau)$ in $H_C^{(0)}$ (recall Eq. 20).

Our next steps are to integrate out the $\theta_{\sigma}(x, \tau)$ -fields and then the $\lambda_{\sigma}(\tau)$ -fields. Once again, only straightforward—albeit tedious—Gaussian integrations are required. To leading order in the perturbative factor $\delta\hat{n}$, the result is an effective action dependent only on the scalar fields $\theta_{\sigma}^{(0)}(\tau)$ and their Fourier transforms $\tilde{\theta}_{\sigma}^{(0)}(\omega)$:

$$\begin{aligned} S_{\theta}^K &= \sum_{\sigma} \int \frac{d\omega}{2\pi} |\omega| \tilde{\theta}_{\sigma}^{(0)}(\omega) \tilde{\theta}_{\sigma}^{(0)}(-\omega) \\ S_{\theta}^C &= \sum_{\sigma_1} \sum_{\sigma_2} \int \frac{d\omega}{2\pi} \left(\frac{U_{\rho}}{\pi} \right) \tilde{\theta}_{\sigma_1}^{(0)}(\omega) \tilde{\theta}_{\sigma_2}^{(0)}(-\omega) \\ S_{\theta}^{(1)} &= \sum_{\sigma_1} \sum_{\sigma_2} \int d\tau \int dx_1 \int dx_2 \int dk_1 \int dk_2 \end{aligned}$$

$$\begin{aligned}
& \times \frac{2U_\rho}{\sqrt{\pi}(2\pi)^3} R(\epsilon_1, \epsilon_2) A(x_1, x_2) \\
& \times \left\{ e^{i\pi\rho/N_{\text{ch}}} \frac{e^{-i[D(\epsilon_2)-D(\epsilon_1)]} e^{-i(k_1x_1+k_2x_2)}}{k_2 - k_1 - i\eta} \right. \\
& \quad \times \theta_{\sigma_2}^{(0)}(\tau) e^{-i \int d\omega h_2(x_1, x_2, \omega)} e^{-i\omega\tau} \tilde{\theta}_{\sigma_1}^{(0)}(\omega) \\
& \quad \left. + \text{m.t.} \right\}, \tag{24}
\end{aligned}$$

where the ‘‘mirror term’’ (m.t.) can be obtained by complex conjugating both the factors that precede $\theta_{\sigma_2}^{(0)}(\tau)$ and the exponential prefactor i that precedes the integral over ω , and where the functions $A(x_1, x_2)$, $h_2(x_1, x_2, \omega)$, $h_1(x_1, x_2, \omega)$, and $h_0(x_1, x_2, \omega)$ are given by the following formulae:

$$\begin{aligned}
A(x_1, x_2) &= \frac{1}{(|x_1| + |x_2| + \alpha)^{1/2}} \\
& \times \frac{1}{(2|x_1| + \alpha)^{1/4} (2|x_2| + \alpha)^{1/4}} \\
& \times \left[\frac{\alpha(2|x_1| + \alpha)^{1/2} (2|x_2| + \alpha)^{1/2}}{(|x_1| + \alpha)(|x_2| + \alpha)} \right]^{1/2} \\
& \times \left[\frac{(|x_1| + \alpha)(|x_2| + \alpha)}{\alpha(|x_1| + |x_2| + \alpha)} \right]^{\text{sgn}(x_1)\text{sgn}(x_2)/2} \\
h_2(x_1, x_2, \omega) &= h_1(x_1, x_2, \omega) - h_0(x_1, x_2, \omega) \\
h_1(x_1, x_2, \omega) &= \text{sgn}(\omega) \frac{\text{sgn}(x_2) [1 - e^{-|\omega x_2|/v_F}]}{2\sqrt{\pi}} \\
& \quad - \{x_1 \leftrightarrow x_2\} \\
h_0(x_1, x_2, \omega) &= \frac{e^{-|\omega x_1|/v_F} + e^{-|\omega x_2|/v_F}}{2\sqrt{\pi}}, \tag{25}
\end{aligned}$$

where ‘‘ $\{x_1 \leftrightarrow x_2\}$ ’’ is the same as the preceding term, except with the roles of x_1 and x_2 reversed.

The effective action of Eq. 24 is the end result for this section. As promised, this action depends only on a single set of scalar fields, which are equivalent to the original θ -fields at $x = 0$. Sections III and IV use this action to solve for the fractional peak splitting f in systems with one and two interdot channels, respectively. In both sections, the general approach is to treat $S_\theta^{(0)} = S_\theta^K + S_\theta^C$ as the unperturbed action and to solve perturbatively in $S_\theta^{(1)}$.

III. FINITE-BARRIER RESULT FOR THE ONE-CHANNEL PROBLEM

Here we consider the single-channel case ($N_{\text{ch}} = 1$), in which electrons of only one spin have enough energy to penetrate into the point contact. Starting with the unperturbed action $S_\theta^{(0)} = S_\theta^K + S_\theta^C$, it is not hard to find that

$$\langle \tilde{\theta}^{(0)}(\omega_1) \tilde{\theta}^{(0)}(\omega_2) \rangle = \frac{\pi}{|\omega_1| + U_\rho/\pi} \delta(\omega_1 + \omega_2). \tag{26}$$

We use this identity to calculate the first-order correction to the ground state energy: $\Delta(\rho) = \langle S_\theta^{(1)} \rangle / \beta$. In particular, we find the following:

$$\begin{aligned}
\Delta(\rho) &= \frac{U_\rho}{(2\pi)^3 \sqrt{\pi}} \int dx_1 \int dx_2 \int dk_1 \int dk_2 R(\epsilon_1, \epsilon_2) \\
& \quad \frac{e^{C_2(x_1, x_2, 2U_\rho)/4}}{(|x_1| + |x_2| + \alpha)^{1/2} (2|x_1| + \alpha)^{1/4} (2|x_2| + \alpha)^{1/4}} \\
& \quad \times e^{-(\pi/2) \int d\omega [h_0(x_1, x_2, \omega)]^2 \frac{e^{-\alpha|\omega|/v_F}}{|\omega| + U_\rho/\pi}} \\
& \quad \times \int d\omega h_0(x_1, x_2, \omega) \frac{e^{-\alpha|\omega|/v_F}}{|\omega| + U_\rho/\pi} \\
& \quad \times \left[i e^{i\pi\rho} \frac{e^{-i[D(\epsilon_2)-D(\epsilon_1)]} e^{-i(k_1x_1+k_2x_2)}}{k_2 - k_1 - i\eta} + \text{c.c.} \right], \tag{27}
\end{aligned}$$

where the function $C_2(x_1, x_2, 2U_\rho)$ is defined below in Eq. 32.

Before we apply standard techniques of complex analysis to reduce the integral over k_2 to the contributions from the simple poles at $k_2 = k_1 \pm i\eta$, we need to show that we can neglect the effects of the singularities in the expression for $S_\theta^{(1)}$ that result from the factors $R(\epsilon_1, \epsilon_2)$ and $D(\epsilon)$. It is not too hard to discount the singular behavior at $\epsilon_2 = 0$ that results from the functional form of $D(\epsilon)$ (see Eq. 13). We can rewrite $\epsilon \ln |\epsilon|$ as follows:

$$\epsilon \ln |\epsilon| = \epsilon \ln \epsilon - i\pi\epsilon \tilde{\Theta}(-\epsilon), \tag{28}$$

where $\tilde{\Theta}(-\epsilon)$ is a sort of variant of the Heaviside step function that, in the appropriate limits, is 1 for ϵ real and negative and is 0 for ϵ real and positive. To allow for complex values of ϵ , we can define $\tilde{\Theta}(-\epsilon)$ by the formula $\tilde{\Theta}(-\epsilon) = \lim_{v \rightarrow 0} \int_{\Gamma(\epsilon)} dz \frac{v}{\pi(z^2 + v^2)}$, where the path $\Gamma(\epsilon)$ in the complex plane starts at $z = R$ (with R being a large and positive real number, ultimately taken to ∞) and then proceeds to the value ϵ by the shortest path that avoids the singularities at $z = \pm iv$ and their accompanying branch cuts. In the limit $R \rightarrow \infty$, this definition yields the desired behavior for real values of ϵ . On the other hand, it does leave $\tilde{\Theta}(-\epsilon)$ with two branch points (at $\epsilon = \pm iv$), and to these we must add the branch point of $\epsilon \ln \epsilon$ at $\epsilon = 0$.

Fortunately, it is not too hard to see that integrating around these singularities and associated branch cuts leads to contributions to the final result that are higher-order in the expansion parameter $2\pi U_\rho / \hbar\omega_P$ than the contributions from the simple poles at $k_2 = k_1 \pm i\eta$. Rough evaluation of the higher-order contributions indicates that they are indeed negligible in the regime where $2\pi U_\rho / \hbar\omega_P \lesssim 2$, but are probably not negligible for values of $2\pi U_\rho / \hbar\omega_P$ approaching 10.

Having discounted higher-order contributions from singularities other than the simple poles at $k_2 = k_1 \pm i\eta$, we can perform the k_2 integral with ease. The integral over k_1 can then be done after the resulting factor $R(\epsilon_1, \epsilon_1)$ is expanded in powers of $e^{\pm\pi\epsilon_1}$ (and after it is noted that $e^{-i[D(\epsilon_1)-D(\epsilon_1)]} = 1$), and the result is the following:

$$\Delta(\rho) = -\frac{2U_\rho}{(2\pi)^2} \cos(\pi\rho) J_1(\epsilon_F, U_\rho, \omega_P), \quad (29)$$

where, once again, ϵ_F is the ‘‘dimensionless Fermi energy’’ relative to the barrier peak, ω_P is the harmonic oscillator energy of the parabolic barrier (recall the discussion of Sec. I), and

$$J_1(\epsilon_F, U_\rho, \omega_P) = \int_{-\infty}^{\infty} dx_1 \int_{-\infty}^{\infty} dx_2 [\Theta(x_1) + \Theta(-x_2)] \times e^{i\epsilon_F \omega_P (x_1 + x_2)/v_F} F_1(x_1, x_2, U_\rho, \omega_P). \quad (30)$$

As before, $\Theta(x)$ is the Heaviside step function and v_F is the Fermi velocity. Furthermore, the function $F_1(x_1, x_2, U_\rho, \omega_P)$ has the formula:

$$F_1(x_1, x_2, U_\rho, \omega_P) = \left(\frac{\omega_P}{2\sqrt{\pi}v_F} \right) \sum_{n=0}^{\infty} (-1)^n \times \frac{2(2n+1)\pi}{(2n+1)^2\pi^2 + (x_1+x_2)^2\omega_P^2/v_F^2} \times \frac{e^{C_2(x_1, x_2, U_\rho)/4}}{(|x_1| + |x_2| + \alpha)^{1/2}} \times \frac{1}{(2|x_1| + \alpha)^{1/4} (2|x_2| + \alpha)^{1/4}} \times e^{-(\pi/2) \int d\omega [h_0(x_1, x_2, \omega)]^2 \frac{e^{-\alpha|\omega|/v_F}}{|\omega| + U_\rho/\pi}} \times \int d\omega h_0(x_1, x_2, \omega) \frac{e^{-\alpha|\omega|/v_F}}{|\omega| + U_\rho/\pi}, \quad (31)$$

where

$$\begin{aligned} C_2(x_1, x_2, U_\rho) &= C_1(x_1, x_2, U_\rho) + C_1(x_2, x_1, U_\rho) \\ C_1(x_1, x_2, U_\rho) &= - \int_0^1 dz \frac{e^{-(\alpha U_\rho/\pi v_F)z}}{z} \\ &\times \left[\left(1 - e^{-(U_\rho|x_1|/\pi v_F)z} \right)^2 \right. \\ &\quad \left. - \text{sgn}(x_1) \text{sgn}(x_2) \left(1 - e^{-(U_\rho|x_2|/\pi v_F)z} \right) \right. \\ &\quad \left. \times \left(1 - e^{-(U_\rho|x_1|/\pi v_F)z} \right) \right] \\ &- 2 \left(e^{U_\rho|x_1|/\pi v_F} - 1 \right) \left(1 - \text{sgn}(x_1) \text{sgn}(x_2) \right) \\ &\quad \times \int_1^\infty dz \frac{e^{-(\alpha+|x_1|)(U_\rho/\pi v_F)z}}{z} \\ &+ \left(e^{2U_\rho|x_1|/\pi v_F} - 1 \right) \\ &\quad \times \int_1^\infty dz \frac{e^{-(\alpha+2|x_1|)(U_\rho/\pi v_F)z}}{z} \\ &- \text{sgn}(x_1) \text{sgn}(x_2) \left(e^{U_\rho(|x_1|+|x_2|/\pi v_F)} - 1 \right) \\ &\quad \times \int_1^\infty dz \frac{e^{-(\alpha+|x_1|+|x_2|)(U_\rho/\pi v_F)z}}{z}. \quad (32) \end{aligned}$$

Although the equation for $\Delta(\rho)$ may not be entirely transparent, it is not hard to confirm, by taking the

limit $\omega_P \rightarrow \infty$, that the result for f that follows from Eqs. 3 and 29 agrees with that previously derived for a delta-function barrier.⁷⁻⁹ The key is to recognize that the relation $\sqrt{1-g} = e^{-\pi\epsilon_F/\sqrt{1+e^{-2\pi\epsilon_F}}}$ means that that $J_1(\epsilon_F, U_\rho, \omega_P) \rightarrow 2e^\gamma \sqrt{1-g}$ as $2\pi U_\rho/\omega_P \rightarrow 0$, where γ is the Euler-Mascheroni constant ($\gamma \simeq 0.577$).

The behavior for $2\pi U_\rho/\hbar\omega_P \neq 0$ can be found through numerical integration. The results for various values of $2\pi U_\rho/\hbar\omega_P$ are displayed in Figure 2. As predicted in our study of the weak-coupling limit ($g \rightarrow 0$),¹⁰ for a given value of g in the vicinity of 1, the fractional peak splitting f is reduced relative to that for a delta-function barrier. This strong-coupling depression of the f -versus- g curve becomes greater for larger values of $2\pi U_\rho/\hbar\omega_P$.

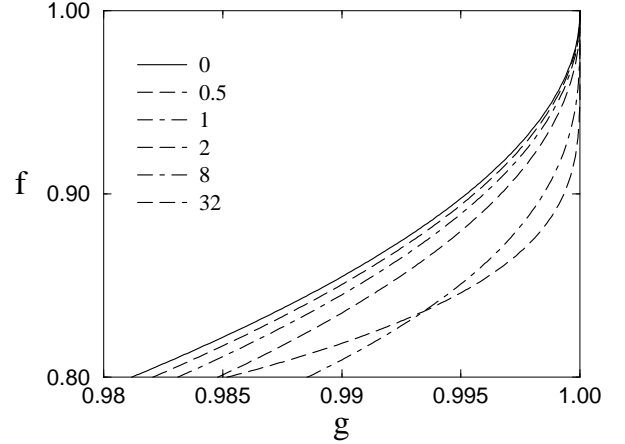


FIG. 2. Plots of the leading $(1-g) \rightarrow 0$ behavior of f , the fractional peak splitting, as a function of g , the dimensionless interdot channel conductance, for a one-channel connection between two quantum dots ($N_{\text{ch}} = 1$). Each curve corresponds to a different value of the quantity $2\pi U_\rho/\hbar\omega_P$ (see legend to the left of the curves). The solid line is the result for an interdot barrier that has effectively zero width ($2\pi U_\rho/\hbar\omega_P = 0$). The dashed and dot-dashed curves show the leading f -versus- g dependence for finite barriers with $2\pi U_\rho/\hbar\omega_P$ taking on values from 0.5 to 32. The curves are expected to be substantially accurate at least for $(1-g)$ greater than or equal to approximately 10^{-3} and for values of $2\pi U_\rho/\hbar\omega_P$ not much larger than 2.

For $2\pi U_\rho/\hbar\omega_P \simeq 1$, however, the downward correction is quite small. Since earlier approximations of the barrier as a delta function were designed to predict the behavior of experimental systems in which $2\pi U_\rho/\hbar\omega_P \simeq 1$,^{1-3,10} our calculation confirms that those prior results were substantially correct. Figure 2 gives a sense of what the leading $2\pi U_\rho/\hbar\omega_P$ -dependent corrections look like for small and large values of $2\pi U_\rho/\hbar\omega_P$, but, because of the approximations we have made, the results are expected to be reliably accurate only for $2\pi U_\rho/\hbar\omega_P \lesssim 2$.

One might wonder what analytic form the leading $2\pi U_\rho/\hbar\omega_P$ -dependent corrections take. In the weak-coupling limit ($g \rightarrow 0$), the finiteness of the barrier was

shown to result in leading-order corrections proportional to $(2\pi U_\rho/\hbar\omega_P)/|\ln g|$ for $2\pi U_\rho/\hbar\omega_P \lesssim 2$.¹⁰ Corrections of this form arose from the fact that transitions into virtual states with energies near or above that of the barrier peak allow for relatively free interdot movement (with transmission probabilities on the order of 1).

By reasoning analogous (but in a sense opposite) to that used in studying the weakly coupled system, we expect that, to leading order, the finite-barrier corrections in the strong-coupling limit, where $(1-g) \ll 1$, are dominated by the enhanced backscattering of states near or below the barrier peak, where reflection probabilities are on the order of 1, rather than on the order of $\sqrt{1-g}$ as is true near the Fermi surface. To estimate these corrections from strongly backscattered states, it is best to return to the form of $\Delta(\rho)$ that appeared in Eq. 27.

Examination of the x -dependent factors in Eq. 27's integrand reveals that the primary contributions for the integral come when the variables x_i have values of rough magnitude $\pi\hbar v_F/2U_\rho$. In this range of x_i -values, the k_i -independent factors of the integrand (i.e., all the factors but $R(\epsilon_1, \epsilon_2)$ and those enclosed in the final set of large brackets) vary relatively slowly, only changing substantially when one or both of the x_i values changes by an addend of order $\pi\hbar v_F/2U_\rho$. Consequently, if the wave vectors k_i have magnitudes greater than $2U_\rho/\pi\hbar v_F$, the k_i -independent factors can, to leading order, be treated as constants for $x_i \sim \pi\hbar v_F/2U_\rho$, and the x_i -dependence of the integrands in Eq. 27 can be assumed to be dominated by the factor $e^{\pm i(k_1 x_1 + k_2 x_2)}$.

The question then is whether the k_i values that contribute most substantially to the $2\pi U_\rho/\hbar\omega_P$ -dependence are large enough (in magnitude) for this assumption to be justified. As we have reasoned above, the leading contributions to $2\pi U_\rho/\hbar\omega_P$ -dependence are expected to come from k_i such that energy of the corresponding eigenstate is near or below the barrier peak. In other words, the most significant wave vectors are expected to be ones such that $E_F + \hbar v_F k_i \lesssim V_0$. Consequently, we expect these k_i to be negative and to have magnitudes approximating $k_0 = (\omega_P/v_F)\epsilon_F$, where (given Eq. 14)

$$k_0 \simeq \frac{\omega_P}{2\pi v_F} |\ln(1-g)|. \quad (33)$$

As noted in Sec. II, the anticipated importance of negative wave vectors of approximate magnitude k_0 (which yield values for ϵ_i equal or near to 0) means that we must have $(1-g) \gtrsim 10^{-3}$ for our general approach to be valid. Our desire to gain a more compact analytic approximation to the leading $2\pi U_\rho/\hbar\omega_P$ -dependent behavior now leads us to impose another requirement: $k_0 \gtrsim 2U_\rho/\pi\hbar v_F$. From Eq. 33, this requirement means that we need $(1-g) \ll e^{-(2/\pi)(2\pi U_\rho/\hbar\omega_P)}$. Combining this upper bound on $(1-g)$ with our previous lower bound, we find that our general approach and the new assumption that we propose to make (that the $e^{\pm i(k_1 x_1 + k_2 x_2)}$ -factors dominate the x_i -dependence of the integrands) are both

valid only if $10^{-3} \lesssim (1-g) \lesssim e^{-(2/\pi)(2\pi U_\rho/\hbar\omega_P)}$. The new assumption therefore allows a useful analytic approximation (i.e., an approximation with a significant range of g values in which it is valid) when $2\pi U_\rho/\hbar\omega_P$ is not much greater than 2. For $2\pi U_\rho/\hbar\omega_P$ values slightly over 10, on the other hand, the assumption's utility "breaks down" entirely, as the room between the upper and lower limits on $(1-g)$ vanishes. Nonetheless, because we have already restricted our attention to $2\pi U_\rho/\hbar\omega_P \lesssim 2$, this "break-down" is of no concern; for the values of $2\pi U_\rho/\hbar\omega_P$ of real interest, our new assumption for the purpose of a compact analytic approximation imposes no more restraint than our initial assumption that $(1-g) \ll 1$.

Having determined that we can assume $e^{\pm i(k_1 x_1 + k_2 x_2)}$ -dominance, we can now proceed with estimating the corrections due to wave vectors in the vicinity of k_0 . Approximation of the integrations based on the above assumptions leads to the conclusion that, to first approximation, the correction to $\Delta(\rho)$ is proportional to $(2\pi U_\rho/\hbar\omega_P)/|\ln(1-g)|$. Thus, the leading finite-barrier correction to the fractional peak splitting f may be roughly written as $-c_1(2\pi U_\rho/\hbar\omega_P)/|\ln(1-g)|$, where c_1 is a small positive number. The form of this correction is parallel to that found in the weak-coupling limit; in both cases, the leading $2\pi U_\rho/\hbar\omega_P$ -dependent terms are proportional to $(2\pi U_\rho/\hbar\omega_P)/|\ln(\frac{1-g}{g})|$. The results displayed in Figure 2 bear out our approximation to the analytic behavior of the leading strong-coupling corrections. The graphed corrections for $0 \leq (2\pi U_\rho/\hbar\omega_P) \leq 2$ agree with the predicted analytic behavior, producing errors of less than about 10% for the behavior as a function of $(1-g)$ and of less than about 20% for the behavior as a function of $2\pi U_\rho/\hbar\omega_P$. The graphed values suggest that the value of c_1 is slightly less than 0.05.

IV. FINITE-BARRIER RESULT FOR THE TWO-CHANNEL PROBLEM

The downward shift of the f -versus- g curve for one-channel systems ($N_{\text{ch}} = 1$) is paralleled by a similar downward shift of the f -versus- g curve for two-channel systems ($N_{\text{ch}} = 2$). However, the route to the two-channel result is less straightforward than the already somewhat tortuous route taken for the single-channel problem, largely due to the fact that we now have to deal with two $\theta_\sigma^{(0)}$ -fields in Eq. 24, rather than just one. The first step in dealing with this set of fields is to transform them to a more manageable pair—the "charge" and "spin" fields θ_C and θ_S , respectively—which are linear combinations of the θ_1 and θ_2 fields: $\theta_C = \theta_1^{(0)} + \theta_2^{(0)}$ and $\theta_S = \theta_1^{(0)} - \theta_2^{(0)}$. The bosonic action S then consists of the sum of separate charge and spin contributions to the unperturbed action S_0 , and a perturbative term S_1 , which depends on both the charge and the spin fields. In particular, $S_0 = S_0^{(C)} + S_0^{(S)}$ and $S = S_0 + S_1$, where

$$\begin{aligned}
S_0^{(C)} &= \int \frac{d\omega}{2\pi} \left(\frac{|\omega|}{2} + \frac{U_\rho}{\pi} \right) \tilde{\theta}_C(\omega) \tilde{\theta}_C(-\omega) \\
S_0^{(S)} &= \int \frac{d\omega}{2\pi} \frac{|\omega|}{2} \tilde{\theta}_S(\omega) \tilde{\theta}_S(-\omega) \\
S_1 &= \frac{2U_\rho}{\sqrt{\pi}(2\pi)^3} \int d\tau \int dx_1 \int dx_2 \int dk_1 \int dk_2 \\
&\times R(\epsilon_1, \epsilon_2) A(x_1, x_2) \\
&\times \left\{ e^{i\pi\rho/2} \frac{e^{-i[D(\epsilon_2)-D(\epsilon_1)]} e^{-i(k_1x_1+k_2x_2)}}{k_2 - k_1 - i\eta} \right. \\
&\quad \times \theta_C(\tau) e^{-(i/2) \int d\omega h_2(x_1, x_2, \omega)} e^{-i\omega\tau} \tilde{\theta}_C(\omega) \\
&\quad + \text{m.t.} \left. \right\} \\
&\times \left\{ e^{-(i/2) \int d\omega h_2(x_1, x_2, \omega)} e^{-i\omega\tau} \tilde{\theta}_S(\omega) + \text{m.t.} \right\}, \quad (34)
\end{aligned}$$

where the “mirror terms” (m.t.) can be obtained in the same way as for Eq. 24.

After integrating out the high-energy charge fields, one is left with an effective spin action $S^{(S)} = S_0^{(S)} + S_1^{(S)}$, where $S_0^{(S)}$ is unchanged from Eq. 34 and where

$$\begin{aligned}
S_1^{(S)} &= \frac{U_\rho}{(2\pi)^3 \sqrt{\pi}} \int_0^\beta d\tau \int dx_1 \int dx_2 \int dk_1 \int dk_2 \\
&\times R(\epsilon_1, \epsilon_2) A(x_1, x_2) e^{C_2(x_1, x_2, 2U_\rho)/8} \\
&\times \left[\frac{\alpha (2|x_1| + \alpha)^{1/2} (2|x_2| + \alpha)^{1/2}}{(|x_1| + \alpha)(|x_2| + \alpha)} \right]^{-1/4} \\
&\times \left[\frac{(|x_2| + \alpha)(|x_1| + \alpha)}{\alpha(|x_1| + |x_2| + \alpha)} \right]^{-\text{sgn}(x_1)\text{sgn}(x_2)/4} \\
&\times e^{-(\pi/4) \int d\omega [h_0(x_1, x_2, \omega)]^2 \frac{e^{-\alpha|\omega|/v_F}}{|\omega| + 2U_\rho/\pi}} \\
&\times \int d\omega h_0(x_1, x_2, \omega) \frac{e^{-\alpha|\omega|/v_F}}{|\omega| + 2U_\rho/\pi} \\
&\times \left[i e^{i\pi\rho/2} \frac{e^{-i[D(\epsilon_2)-D(\epsilon_1)]} e^{-i(k_1x_1+k_2x_2)}}{k_2 - k_1 - i\eta} + \text{c.c.} \right] \\
&\times \left[e^{-(i/2) \int d\omega h_2(x_1, x_2, \omega)} e^{-i\omega\tau} \tilde{\theta}_S(\omega) + \text{m.t.} \right], \quad (35)
\end{aligned}$$

where, as was done in the case of the $N_{\text{ch}} = 1$ problem, only the lowest-order perturbative term has been retained in the effective action.

To exploit the even-odd combinations that occur in the integrals over ω , we rewrite the action in terms of the following “even” and “odd” fields:

$$\begin{aligned}
\tilde{\theta}_S^{(E)} &= e^{-i\omega\tau} \tilde{\theta}_S(\omega) + e^{i\omega\tau} \tilde{\theta}_S(-\omega) \\
\tilde{\theta}_S^{(O)} &= i \left[e^{-i\omega\tau} \tilde{\theta}_S(\omega) - e^{i\omega\tau} \tilde{\theta}_S(-\omega) \right]. \quad (36)
\end{aligned}$$

The nonperturbative term $S_0^{(S)}$ then takes the form

$$\begin{aligned}
S_0^{(S)} &= \frac{1}{4} \int_0^\infty \frac{d\omega}{2\pi} \omega \left[\tilde{\theta}_S^{(E)}(\omega, \tau) \tilde{\theta}_S^{(E)}(\omega, \tau) \right. \\
&\quad \left. + \tilde{\theta}_S^{(O)}(\omega, \tau) \tilde{\theta}_S^{(O)}(\omega, \tau) \right]. \quad (37)
\end{aligned}$$

After integrating out the $\tilde{\theta}_S^{(O)}$ -fields, we have a new effective action in terms of the $\tilde{\theta}_S^{(E)}$ -fields.

The “even” fields are not to be left alone, however. In anticipation of “refermionization,” we insert into the effective action a set of dummy “odd” fields—free fields that are entirely decoupled from the “even” fields. The nonperturbative, kinetic energy terms of these new $\tilde{\theta}_S^{(O)}$ -fields and $\tilde{\theta}_S^{(E)}$ -fields add to give a total kinetic energy of the same form as that in Eq. 37. This total is in turn rewritten in a form equivalent to that of $S_0^{(S)}$ in Eq. 34. Our newest, and final, effective action then consists of the sum of this $S_0^{(S)}$ -term and the leading perturbative term S_1^f , which was derived from integrating out the original “odd” fields:

$$\begin{aligned}
S_1^f &= \frac{U_\rho}{(2\pi)^3 \sqrt{\pi}} \int_0^\beta d\tau \int dx_1 \int dx_2 \int dk_1 \int dk_2 \\
&\times \frac{R(\epsilon_1, \epsilon_2) e^{C_2(x_1, x_2, 2U_\rho)/8}}{(|x_1| + |x_2| + \alpha)^{1/2} (2|x_1| + \alpha)^{1/4} (2|x_2| + \alpha)^{1/4}} \\
&\times e^{-(\pi/4) \int d\omega [h_0(x_1, x_2, \omega)]^2 \frac{e^{-\alpha|\omega|/v_F}}{|\omega| + 2U_\rho/\pi}} \\
&\times \int d\omega h_0(x_1, x_2, \omega) \frac{e^{-\alpha|\omega|/v_F}}{|\omega| + 2U_\rho/\pi} \\
&\times \left[i e^{i\pi\rho/2} \frac{e^{-i[D(\epsilon_2)-D(\epsilon_1)]} e^{-i(k_1x_1+k_2x_2)}}{k_2 - k_1 - i\eta} + \text{c.c.} \right] \\
&\times \left[e^{(i/2) \int d\omega h_0(x_1, x_2, \omega)} e^{-i\omega\tau} \tilde{\theta}_S(\omega) + \text{m.t.} \right]. \quad (38)
\end{aligned}$$

As in prior work,^{5,9} we “refermionize” the bosonic action $S = S_0^{(S)} + S_1^f$ by identifying $\psi_f(0, \tau)$ as a fermionic annihilation operator at the origin of a semi-infinite system, where

$$\psi_f(0, \tau) = \frac{e^{-(i/2) \int d\omega h_0(x_1, x_2, \omega)} e^{-i\omega\tau} \tilde{\theta}_S(\omega)}{\sqrt{2\pi} \tilde{\alpha}(x_1, x_2)}, \quad (39)$$

where

$$\tilde{\alpha}(x_1, x_2) = (2|x_1| + \alpha)^{1/4} (2|x_2| + \alpha)^{1/4} (|x_1| + |x_2| + \alpha)^{1/2}. \quad (40)$$

This refermionization formula may look peculiar because of its use of a normalization factor and an ultraviolet cutoff (embedded in $h_0(x_1, x_2, \omega)$) that depend on position variables, rather than mere constants (contrast the standard bosonic representation of fermionic position operators in Eq. 7). These position-dependent factors work, in tandem with the scalar prefactor ($i/2$) for the exponentiated integral, to ensure the correct anticommutation relations for $\psi_f(0, \tau)$, and their use is expected to be unobjectionable so long as for all x_i of real interest the resulting ultraviolet cutoff is high enough to capture the behavior with which we are concerned.

As in the single-channel problem, the x_i of real interest satisfy $|x_i| \sim \pi \hbar v_F / 2U_\rho$ (as can be seen by doing the integrals over k_i and obtaining a result with factors analogous

to those of $F_1(x_1, x_2, U_\rho, \omega_P)$ of Eq. 31). The ultraviolet cutoffs in Eq. 39 therefore characteristically correspond to energies approximating $2U_\rho/\pi$ —which is much greater than $k_B T$, the characteristic energy for the unperturbed spin degrees of freedom, and (as we can confirm once we rediscover the leading order behavior produced by S_1^f), much greater than the energy of states characteristically brought into play by the perturbation S_1^f . Indeed, we have already incorporated an assumption that ultraviolet cutoffs approximating $2U_\rho/\pi$ are valid because, in obtaining our effective action, we have only kept the leading order terms from integrating out the charge degrees of freedom—an approximation only expected to be good if the spin-field states of concern have excitation energies significantly less than U_ρ .⁵

Returning to Eq. 38, we use the identity $\sqrt{2\pi} \int_0^\beta d\tau [\psi_f(0, \tau) + \psi_f^\dagger(0, \tau)] = \int dk (f_k^\dagger + f_k)$ to find that our refermionization scheme produces a fermionic Hamiltonian $H = H_0 + H_1$ that consists of the following parts:

$$\begin{aligned} H_0 &= \int dk \xi_k f_k^\dagger f_k \\ H_1 &= Z(\epsilon_F, U_\rho, \rho) \int dk (f_k^\dagger + f_k), \end{aligned} \quad (41)$$

where

$$\begin{aligned} Z(\epsilon_F, U_\rho, \omega_P, \rho) &= \frac{U_\rho}{(2\pi)^3 \sqrt{\pi}} \int dx_1 \int dx_2 \int dk_1 \int dk_2 \\ &\times \frac{R(\epsilon_1, \epsilon_2) e^{C_2(x_1, x_2, 2U_\rho)/8}}{(|x_1| + |x_2| + \alpha)^{1/4} (2|x_1| + \alpha)^{1/8} (2|x_2| + \alpha)^{1/8}} \\ &\times e^{-(\pi/4) \int d\omega [h_0(x_1, x_2, \omega)]^2 \frac{e^{-\alpha|\omega|/v_F}}{|\omega| + 2U_\rho/\pi}} \\ &\times \int d\omega h_0(x_1, x_2, \omega) \frac{e^{-\alpha|\omega|/v_F}}{|\omega| + 2U_\rho/\pi} \\ &\times \left[i e^{i\pi\rho/2} \frac{e^{-i[D(\epsilon_2) - D(\epsilon_1)]} e^{-i(k_1 x_1 + k_2 x_2)}}{k_2 - k_1 - i\eta} + \text{c.c.} \right]. \end{aligned} \quad (42)$$

From prior work on the effects of a delta-function barrier, we know how to solve for the fractional peak splitting that such a Hamiltonian produces.⁷⁻⁹ The only difference from the delta-function barrier Hamiltonian that we encountered before is that a complicated prefactor $Z(\epsilon_F, U_\rho, \omega_P, \rho)$ replaces the simpler delta-function barrier prefactor $Z_\infty(\epsilon_F, U_\rho, \rho) = \cos(\pi\rho/2) \sqrt{1-g} \sqrt{2e^\gamma \hbar v_F U_\rho / \pi^3}$, where γ is the Euler-Mascheroni constant ($\gamma \simeq 0.577$).⁷⁻⁹ Thus, to find the leading behavior of the fractional peak splitting as a function of $(1-g)$ and $2\pi U_\rho/\hbar\omega_P$, we can simply substitute $Z(\epsilon_F, U_\rho, \omega_P, \rho)$ for $Z_\infty(\epsilon_F, U_\rho, \rho)$ in the results previously obtained for a delta-function barrier.

As for one-channel systems, we ultimately resort to numerical integration to solve for the fractional peak splitting when the barrier has a nonzero width. Needless to say, it is gratifying that such numerical calculation confirms that, at least through five significant digits, the

prefactor $Z(\epsilon_F, U_\rho, \omega_P, \rho)$ converges to the delta-function quantity $Z_\infty(\epsilon_F, U_\rho, \rho)$ in the limit $2\pi U_\rho/\hbar\omega_P \rightarrow 0$. Consequently, in the limit of a narrow barrier, we recover the same result as for a delta-function barrier⁷⁻⁹—a good confirmation both of the robustness of our earlier results and of our success in wending through the complications created by the initial assumption of a nonzero-width barrier.

The approach to performing the quadruple integral of Eq. 42 is very similar to that used to perform the analogous quadruple integral for $N_{\text{ch}} = 1$ and therefore will not be described in depth. We first integrate over k_1 and k_2 by techniques of complex analysis similar to those used for $N_{\text{ch}} = 1$, once again focusing on the simple poles at $k_2 = k_1 \pm i\eta$, with the understanding that this imposes a constraint that $2\pi U_\rho/\hbar\omega_P \lesssim 2$. For various values of $2\pi U_\rho/\hbar\omega_P$, we then do the remaining integrals over x_1 and x_2 numerically. The results are shown in Figure 3. As for one-channel systems, we see that as $2\pi U_\rho/\hbar\omega_P$ increases, the strong-coupling end of the f -versus- g curve shifts downward from the zero-width result. Once again, the corrections for the experimentally realized values of $2\pi U_\rho/\hbar\omega_P \simeq 1$ are small, a fact which confirms that the previous assumption of a delta-function barrier⁷⁻¹⁰ was substantially justified, at least so long as interaction effects peculiar to the barrier region can be ignored.

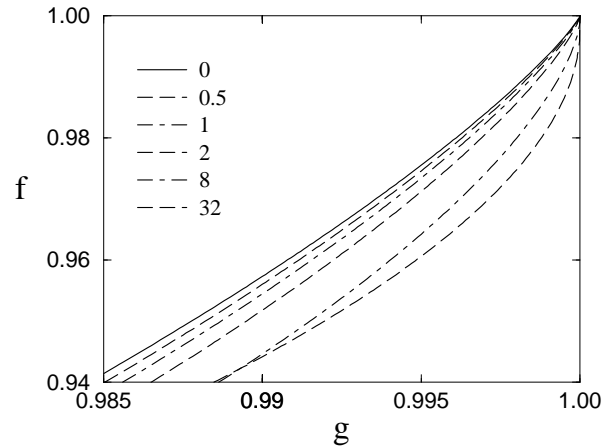


FIG. 3. Plots of the leading $(1-g) \rightarrow 0$ behavior of f , the fractional peak splitting, as a function of g , the dimensionless interdot channel conductance, for a two-channel connection between two quantum dots ($N_{\text{ch}} = 2$). Each curve corresponds to a different value of the quantity $2\pi U_\rho/\hbar\omega_P$ (see legend to the left of the curves). The solid line is the result for an interdot barrier that has effectively zero width ($2\pi U_\rho/\hbar\omega_P = 0$). The dashed and dot-dashed curves show the leading f -versus- g dependence for finite barriers with $2\pi U_\rho/\hbar\omega_P$ taking on values from 0.5 to 32. The curves are expected to be substantially accurate at least for $(1-g)$ greater than or equal to approximately 10^{-3} and for values of $2\pi U_\rho/\hbar\omega_P$ not much larger than 2.

As for the single-channel system, one might inquire about the nature of the leading analytic behavior of these corrections. The answer is essentially parallel, both in reasoning and substance, to that found at the end of Sec. III. The constraints on $(1 - g)$ are the same (i.e., $10^{-3} \lesssim (1 - g) \ll e^{-(2/\pi)(2\pi U_\rho/\hbar\omega_P)}$), and the leading finite-barrier corrections to $Z(\epsilon_F, U_\rho, \omega_P, \rho)$ are expected to be roughly proportional to $(2\pi U_\rho/\hbar\omega_P)/|\ln(1 - g)|$ when $2\pi U_\rho/\hbar\omega_P \lesssim 2$. In other words, $Z(\epsilon_F, U_\rho, \omega_P, \rho)$ can be expanded as follows:

$$\frac{Z(\epsilon_F, U_\rho, \omega_P, \rho)}{\cos(\pi\rho/2)\sqrt{2e^\gamma\hbar v_F U_\rho/\pi^3}} = \sqrt{1 - g} + c_2 \frac{2\pi U_\rho/\hbar\omega_P}{|\ln(1 - g)|} + \dots, \quad (43)$$

where c_2 is a small positive number. Because, from prior work,⁷⁻⁹ the leading corrections to the fractional peak splitting are proportional to $Z(\epsilon_F, U_\rho, \omega_P, \rho)^2 \ln Z(\epsilon_F, U_\rho, \omega_P, \rho)$ at $\rho = 0$, the leading finite-barrier correction to the fractional peak splitting is roughly proportional to $(2\pi U_\rho/\hbar\omega_P) \sqrt{1 - g} \{1 - |\ln(1 - g)|^{-1}\}$. The corrections shown in Figure 3 follow this predicted behavior quite well: for $2\pi U_\rho/\hbar\omega_P \leq 2$, the analytic prediction captures the calculated corrections with error margins of about 10% or less for the $(1 - g)$ -dependence and of about 20% or less for the $2\pi U_\rho/\hbar\omega_P$ -dependence. The numerical results suggest that c_2 is slightly less than 0.02.

V. CONCLUSION

This paper shows that bosonization techniques for studying the behavior of one-dimensional systems need not be abandoned when finite-length barriers (or constrictions) are introduced. The finite-length effects of those barriers can be captured to leading order by a standard perturbative approach, albeit one that requires complicated calculations and a fair degree of care. Thus, bosonization techniques can still be useful when nontrivial behavior in the barrier region is at issue, and the approach presented in this paper may help investigators to distinguish between single-particle and many-particle effects from a barrier's finite length.

With regard to the more particular problem of the Coulomb blockade behavior of coupled quantum dots, our results can be summarized as follows. This paper shows that at least for one-channel or two-channel systems, the fractional peak splitting f of two strongly coupled dots decreases, for a given value of the interdot conductance, as the ratio $2\pi U_\rho/\hbar\omega_P$ is increased. For one-channel systems ($N_{\text{ch}} = 1$), the downward correction behaves as $(2\pi U_\rho/\hbar\omega_P)/|\ln(1 - g)|$ in the limit where $2\pi U_\rho/\hbar\omega_P \lesssim 2$ and $(1 - g) \ll 1$. Thus, for $N_{\text{ch}} = 1$, the fractional peak splitting has the following leading-order functional form:

$$f_1 = 1 - c_{1,1}\sqrt{1 - g} - c_{1,2} \frac{(2\pi U_\rho/\hbar\omega_P)}{|\ln(1 - g)|}, \quad (44)$$

where $c_{1,2}$ is somewhat less than 0.05 and, as derived in prior work,⁷⁻⁹ $c_{1,1} = 8e^\gamma/\pi^2$ (about 1.44). In two-channel systems ($N_{\text{ch}} = 2$), and in the same limits, the downward correction due to the finite barrier width behaves as $(2\pi U_\rho/\hbar\omega_P) \sqrt{1 - g} \{1 - |\ln(1 - g)|^{-1}\}$, resulting in leading-order behavior of the form

$$f_2 = 1 - c_{2,1}(1 - g)|\ln(1 - g)| - c_{2,2}(2\pi U_\rho/\hbar\omega_P) \sqrt{1 - g} \left\{1 - \frac{1}{|\ln(1 - g)|}\right\}, \quad (45)$$

where $c_{2,2}$ is somewhat less than 0.04 and, as derived in prior work,⁷⁻⁹ $c_{2,1} = 16e^\gamma/\pi^3$ (or about 0.919). (It should be noted that prior results indicate that, in the $N_{\text{ch}} = 2$ equation, the next additive term independent of $2\pi U_\rho/\hbar\omega_P$ will equal $-c_{2,3}(1 - g)$, where $c_{2,3} \simeq 0.425$.⁹ Because this term linear in $(1 - g)$ comes from higher-order terms in the effective action than those we have considered here (see, e.g., Eq. 38), we have omitted it in our calculations and in the graphs of Figure 3 in order to have a truer comparison between the $2\pi U_\rho/\hbar\omega_P$ -dependent terms and those they directly correct. If need be, the linear term is easy enough to combine with the result expressed in Eq. 45.)

The above results combine with an earlier study of the weak-coupling regime ($g \ll 1$)¹⁰ to give a more complete understanding of the f -versus- g curve when one leaves the delta-function barrier limit $2\pi U_\rho/\hbar\omega_P \rightarrow 0$. In particular, we come to the nontrivial conclusion that, for the experimentally realized values of $2\pi U_\rho/\hbar\omega_P \simeq 1$,^{1-3,10} the corrections to the results derived from modeling the barrier as a delta function are not fundamentally substantial; thus, to this extent at least, earlier theoretical work using a delta-function potential was correct.

In addition to confirming the essential nature of the f -versus- g curve for $2\pi U_\rho/\hbar\omega_P \lesssim 2$, this paper has helped us gain a better picture of what happens to the f -versus- g curve for more general values of $2\pi U_\rho/\hbar\omega_P$. The weak-coupling results suggested that, as $2\pi U_\rho/\hbar\omega_P$ is increased, the f -versus- g curve shifts upward for small values of g (i.e., for $g \ll 1$) and becomes flatter for intermediate values of g . The strong-coupling results suggest (as conjectured) that, as the same ratio is increased, the f -versus- g curve shifts downward for large values of g (i.e., for $(1 - g) \ll 1$) and becomes flatter for intermediate values of g . Together, the two sets of results suggest that, in the limit of an extremely wide, "adiabatic" barrier ($2\pi U_\rho/\hbar\omega_P \rightarrow \infty$), the f -versus- g curve will be essentially flat for values of g in an intermediate region between 0 and 1. For such an adiabatic barrier, the f -versus- g curve will sit at some essentially constant value of f for most of this interval and will turn sharply toward the limiting values of $f = 0$ and $f = 1$ at the edges.

For the moment, the intermediate value at which the "adiabatic" f -versus- g curve sits remains a mystery. The weak-coupling results displayed an antisymmetry around

$g = 1/2$ that, if true at higher orders, might aid in solving for the fractional peak splitting when g takes on intermediate values.¹⁰ Unfortunately, the strong-coupling results do not exhibit such a simple symmetry. As Figures 1 and 2 indicate, unlike the weak-coupling results, the strong-coupling results do not reveal a common point of intersection for the leading-order curves that correspond to different values of $2\pi U_\rho/\hbar\omega_P$. The apparent lack of a common pivot will presumably make solution of the intermediate- g problem more difficult.

ACKNOWLEDGMENTS

This work was supported by NSF grants No. DMR99-81283 and No. DMR98-09363, and DARPA grant No. 1034315. The authors thank R. Westervelt, C.H. Crouch, and C. Livermore for helpful conversations.

-
- ¹ F. R. Waugh, M. J. Berry, D. J. Mar, R. M. Westervelt, K. L. Campman, and A. C. Gossard, Phys. Rev. Lett. **75**, 705 (1995); F. R. Waugh, M. J. Berry, C. H. Crouch, C. Livermore, D. J. Mar, R. M. Westervelt, K. L. Campman, and A. C. Gossard, Phys. Rev. B **53**, 1413 (1996); F. R. Waugh, Ph.D. thesis, Harvard University, 1994.
- ² C. H. Crouch, C. Livermore, F. R. Waugh, R. M. Westervelt, K. L. Campman, and A. C. Gossard, Surf. Sci. **361-362**, 631 (1996).
- ³ C. Livermore, C. H. Crouch, R. M. Westervelt, K. L. Campman, and A. C. Gossard, Science **274**, 1332 (1996).
- ⁴ K. Flensberg, Physica B **203**, 432 (1994); Phys. Rev. B **48**, 11 156 (1993).
- ⁵ K. A. Matveev, Phys. Rev. B **51**, 1743 (1995).
- ⁶ L. W. Molenkamp, K. Flensberg, and M. Kemerink, Phys. Rev. Lett. **75**, 4282 (1995).
- ⁷ K. A. Matveev, L. I. Glazman, and H. U. Baranger, Phys. Rev. B **53**, 1034 (1996); **54**, 5637 (1996).
- ⁸ J. M. Golden and B. I. Halperin, Phys. Rev. B **53**, 3893 (1996).
- ⁹ J. M. Golden and B. I. Halperin, Phys. Rev. B **54**, 16 757 (1996).
- ¹⁰ J. M. Golden and B. I. Halperin, Phys. Rev. B **56**, 4716 (1997).
- ¹¹ Y.-L. Liu, Phys. Rev. B **56**, 6732 (1997). Unfortunately, we have not been able to follow the reasoning of Liu's paper, which reports results that contrast sharply with our results here and with those derived in Refs. 7-10.
- ¹² It should be noted that the two-dot system that we have described has a close mathematical relation to other systems, including one consisting of a single dot coupled to one lead through a nearly open point contact. See Refs. 7 and 8 above. Information about the energy of this single dot can be obtained by measuring the capacitance between the dot and a nearby overlying gate. See Ref. 5 above.
- ¹³ K. J. Thomas, J. T. Nicholls, M. Pepper, W. R. Tribe, M. Y. Simmons, and D. A. Ritchie, Phys. Rev. B **61**, R13,365 (2000); K. J. Thomas, J. T. Nicholls, N. J. Appleyard, M. Y. Simmons, M. Pepper, D. R. Mace, W. R. Tribe, and D. A. Ritchie, Phys. Rev. B **58**, 4846 (1998).
- ¹⁴ V. J. Emery, "Theory of the One-Dimensional Electron Gas," in *Highly Conducting One-Dimensional Solids*, edited by J. T. Devreese, R. P. Evrard, and V. E. van Doren (Plenum, New York, 1979), pp. 247-303.
- ¹⁵ R. Heidenreich, R. Seiler, and D. A. Uhlenbrock, J. Stat. Phys. **22**, 27 (1980).
- ¹⁶ F. D. M. Haldane, Phys. Rev. Lett. **47**, 1840 (1981); J. Phys. C **14**, 2585 (1981).
- ¹⁷ E. Fradkin, *Field Theories of Condensed Matter Systems* (Addison-Wesley, Reading, 1991), pp. 74-88.
- ¹⁸ H. J. Schulz, in *Strongly Correlated Electronic Materials: The Los Alamos Symposium, 1993*, edited by K. Bedell et al. (Addison-Wesley, Reading, Massachusetts, 1994), pp. 187ff.; in *Mesoscopic Quantum Physics, Les Houches, Session LXI, 1994*, edited by E. Akkermans, G. Montambaux, J.-L. Pichard, and J. Zinn-Justin (Elsevier, Amsterdam, 1995), pp. 533ff.
- ¹⁹ R. Shankar, Acta Phys. Pol. B **26**, 1835 (1996).
- ²⁰ C. L. Kane and M. P. A. Fisher, Phys. Rev. Lett. **68**, 1220 (1992); Phys. Rev. B **46**, 7268 (1992); **46**, 15 233 (1992).
- ²¹ S. Lal, S. Rao, and D. Sen, Phys. Rev. Lett. **87**, 026801 (2001).
- ²² M. Büttiker, Phys. Rev. B **41**, 7906 (1990).
- ²³ Because we are only concerned with the movement of electrons through the channel between the dots (rather than motion within the dots themselves), we use free boundary conditions, and the eigenfunctions that result consist of incident, transmitted, and reflected parts.
- ²⁴ J. N. L. Connor, Mol. Phys. **15**, 37 (1968).
- ²⁵ J. C. P. Miller in *Handbook of Mathematical Functions*, edited by M. Abramowitz and I. A. Stegun (National Bureau of Standards, Washington, D.C., 1964), Appl. Math. Ser. 55, p. 685.